Synthesis and Drug-Delivery Behavior of Chitosan-Functionalized Graphene Oxide Hybrid Nanosheets

ARTICLE *in* MACROMOLECULAR MATERIALS AND ENGINEERING · FEBRUARY 2011

Impact Factor: 2.66 · DOI: 10.1002/mame.201000307

9 AUTHORS, INCLUDING:

Myeon-Cheon Choi
Pusan National University
30 PUBLICATIONS **668** CITATIONS
SEE PROFILE

Sun-Hee Kim
Pusan National University
49 PUBLICATIONS **745** CITATIONS
SEE PROFILE

Satyendra Mishra
North Maharashtra University
183 PUBLICATIONS **1,590** CITATIONS
SEE PROFILE

Raj Pal Singh
Bharati Vidyapeeth University
142 PUBLICATIONS **2,681** CITATIONS
SEE PROFILE

ISSN 1438-7492 · MMENFA 296 (2) 97–192 (2011) · Vol. 296 · No. 2 · February 14, 2011 D 51047

Macromolecular Materials and Engineering

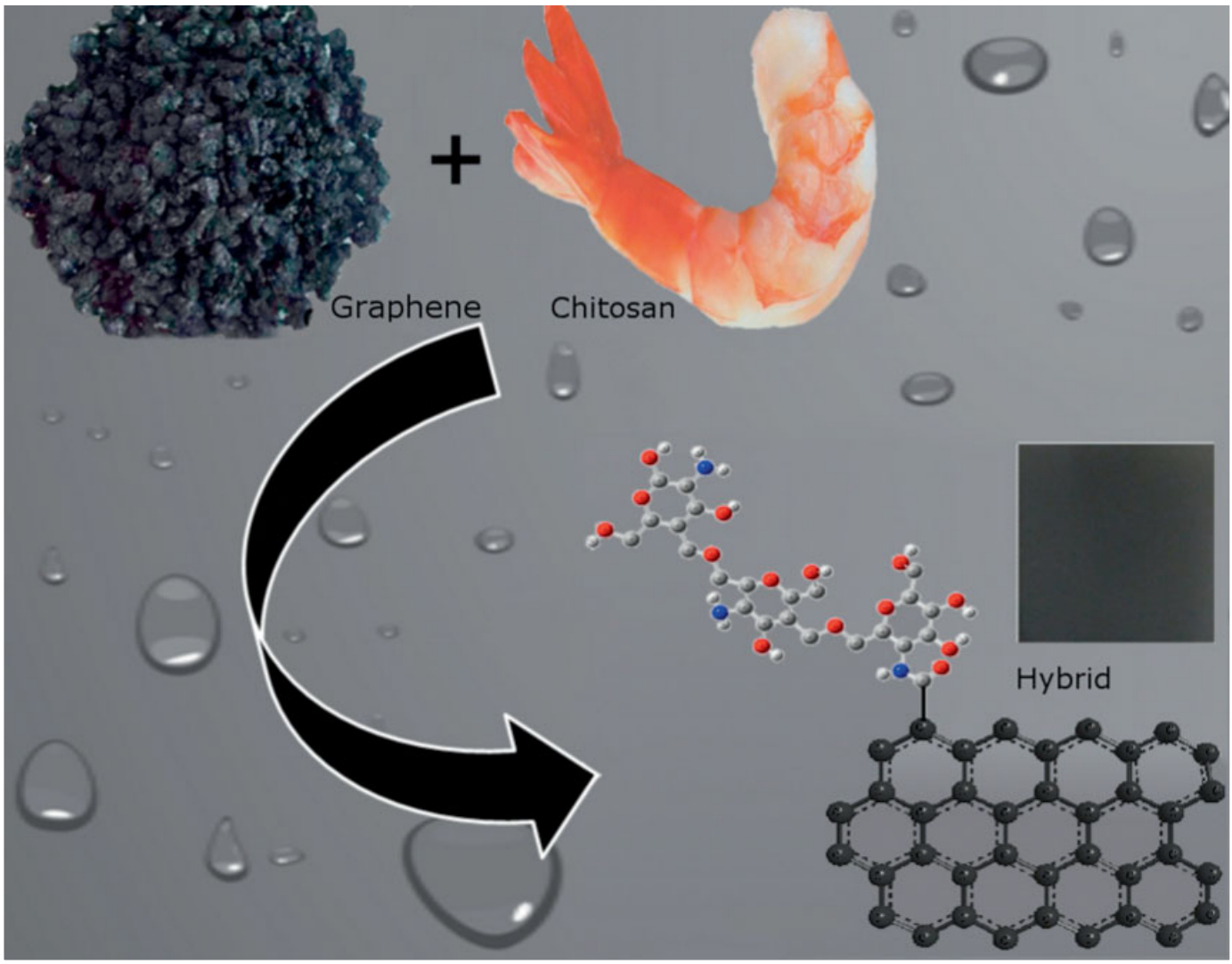

2/2011

WILEY-VCH

Synthesis and Drug-Delivery Behavior of Chitosan-Functionalized Graphene Oxide Hybrid Nanosheets[a]

Vijay Kumar Rana, Myeon-Cheon Choi, Jin-Yeon Kong, Gwang Yeon Kim, Mi Ju Kim, Sun-Hee Kim, Satyendra Mishra, Raj Pal Singh, Chang-Sik Ha*

Chitosan-functionalized graphene oxides (FGOCs) were successfully synthesized. FGOCs were found to significantly improve the solubility of the GO in aqueous acidic media. The presence of organic groups was confirmed by means of XPS and TGA. Restoration of the sp^2 carbon network and exfoliation of graphene sheets were confirmed by Raman spectroscopy, UV-visible spectroscopy and WAXD. The SEM and AFM investigations of the resultant FGOCs showed that most of the graphene sheets were individual and few were layered. Controlled release behavior of Ibuprofen and 5-fluorouracil was then investigated. We found that FGOCs are a promising new material for biological and medical applications.

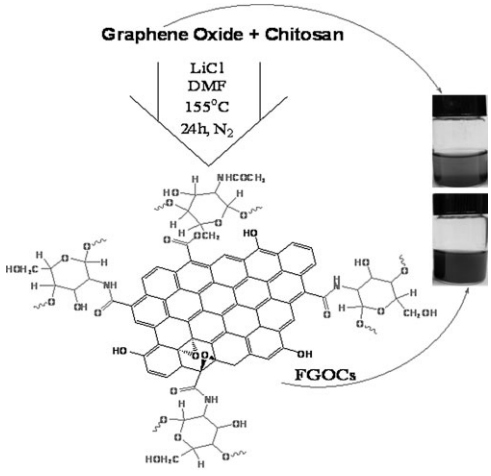

Introduction

Graphene sheets, which are one atom thick and a 2D layer that is entirely made of carbon, have been an extensive research material over the past decade. A single sheet of sp^2-bonded carbon arranges in a honeycomb lattice, with interesting physical and electronic properties.[1,2] Its extraordinary properties, such as high carrier mobility, half-integer quantum Hall effect at room temperature,[3,4] spin transport,[5] high elasticity,[6] electromechanical modulation and ferromagnetism,[7] have made graphene a very promising candidate as a robust atomic-scale scaffold in the design of new nanomaterials.[8] The fracture strength is comparable to fullerenes and carbon nanotubes (CNTs) with similar types of defects.[9] However, like C_{60} and CNTs, graphene tends to aggregate in solution and in the solid state, giving rise to great technical difficulties during the fabrication of graphene-based devices in organic solvents. These aggregates are driven by the enhanced van der Waals attractive forces between graphene sheets. Graphene oxide, prepared by the chemical oxidization of graphite, possesses various reactive functional groups, including hydroxyl, epoxy and carboxylic acid groups. The reactive oxygen

V. K. Rana, M.-C. Choi, J.-Y. Kong, G. Y. Kim, C.-S. Ha
Department of Polymer Science and Engineering, Pusan National University, Geumjeong-gu, Busan 609-735, Korea
Fax: +82 51 514 4331; E-mail: csha@pnu.edu
M. J. Kim, S.-H. Kim
Department of Biochemistry, School of Medicine, Pusan National University, Yangsan 626-870, South Korea
S. Mishra
Department of Chemical Technology, North Maharastra University, Jalgaon 425001, India
R. P. Singh
Division of Polymer Science and Engineering, National Chemical Laboratory, Dr. Homi Bhabha Road, Pune 411 008, India

[a] Supporting information for this article is available at the bottom of the article's abstract page, which can be accessed from the journal's homepage at http://www.mme-journal.de, or from the author.

DOI: 10.1002/mame.201000307

functional groups of graphene oxide (GO) can help GO exfoliated in various solvents to produce homogeneous colloidal suspensions, while influencing the properties of graphene-based materials. One smart behavior of graphene is controlled drug delivery based on non/covalent dynamic bonding interactions, e.g., hydrogen bonding, hydrophobic, π-π stacking and electrostatic interactions, which respond to stimuli release by pH, temperature, ultraviolet or visible lights, chemical substances or electric fields.[10–12] Moreover, graphene sheets as a drug carrier are interesting because both sides of a single sheet could be accessible for drug binding. So far, rational functionalization chemistry has focused on imparting graphene with aqueous solubility and biocompatibility.[10] However, multifunctional graphene hybrid materials that take advantage of both the superior biological properties of graphene and various inherent properties of a functionalizing material have been largely unexplored. The polymer functionalization strategy is not only an effective way to solubilize graphene sheets in water, but this technique is also particularly important for the preparation of polymeric carbon packaging, metal-ion adsorption, novel drug delivery and gene composites. Furthermore, covalent techniques can be used to combine different polymers with graphene in order to create new hybrid materials with desirable properties.[11,12] Thus far, little has been done to explore graphene in biological systems.[13,14] Chitosan (CS) is a biocompatible, biodegradable and non-toxic natural polymer and has applications in wound healing, tissue repair, anti-microbial resistance, cell adhesion and food delivery.[15] Recently, a few reports were presented on CS/GO hybrid systems with enhanced mechanical properties.[16,17] No report has been published so far, however, on biological applications of the CS/GO hybrid systems.

Herein, we demonstrate the biocompatibility and the drug release behavior of covalently CS-functionalized graphene (FGOCs; see Scheme 1). We evaluate the controlled release behavior of two drug molecules, i.e., ibuprofen (IBU) and 5-fluorouracil (5-FU), from the FGOCs. It is considered that the biological application of FGOCs is strongly dependent on the structural and physical characteristics of drugs. For example, the release behavior of drugs having a large molecular structure, e.g., doxorubicin, 7-ethyl-10-hydroxy-camptothecin (SN38) and camptothecin (CPT) etc.

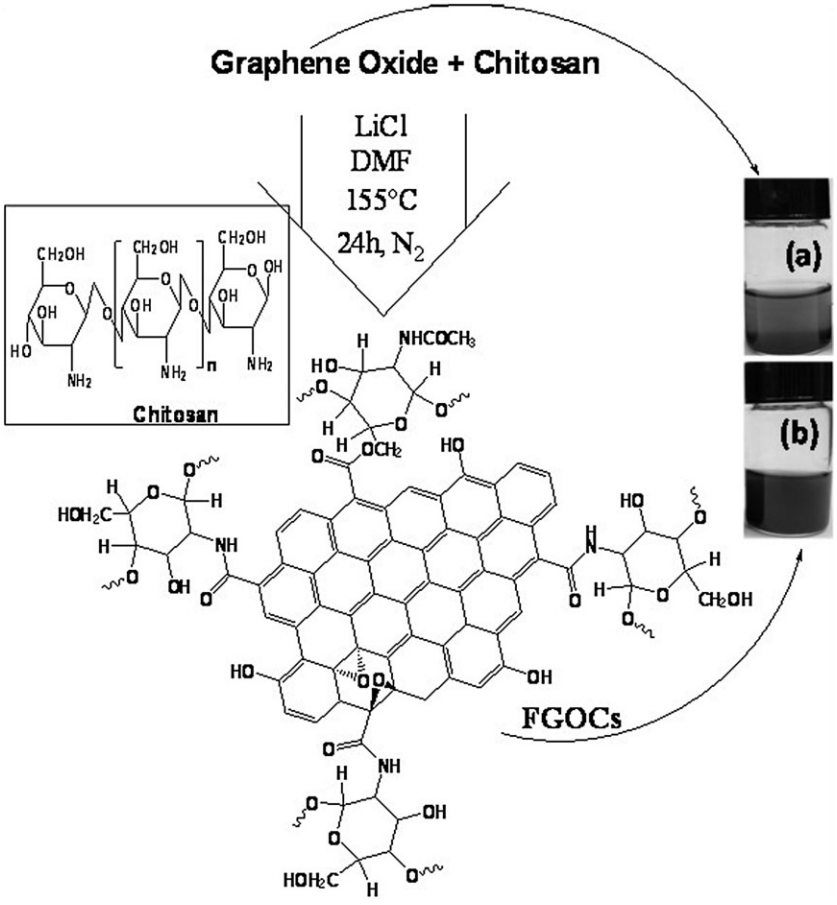

Scheme 1. Synthesis of the FGOCs and the dispersion of (a) GO and (b) the FGOCs in an aqueous acetic acid solution (CH_3COOH/H_2O 0.2/1). More details on the synthesis and characterization of FGOCs are given in the Supporting Information.

from FGOCs nanosheets is different from the two small molecular drugs. We have chosen the two drugs used here based on their different affinity with FGOCs; IBU may have a higher attraction to FGOCs sheets because of its hydrophobic nature with a complete benzene ring (presumably higher π-stacking), while 5-FU has less attraction due to its hydrophilic nature and its diamide group that would contribute in the resonance of the benzenoid (presumably less π-stacking). We expect that the biocompatible FGOCs graphene sheets will be a novel promising material for biological applications. Infrared spectroscopy (FT-IR), thermogravimetric analysis (TGA), and X-ray photoelectron spectroscopy (XPS) confirmed the functionalization of graphene with chitosan and the exfoliation of FGOCs. The restoration of the sp^2 carbon network on the basal planes of the graphene sheets was confirmed by Raman spectroscopy and wide-angle X-ray diffraction (WAXD). Moreover, the low cost, large scale production of graphite and chitosan is unmatched by any hardcore carbon metals and polymers. In short, chitosan functionalized graphene sheets with a stable suspension in an aqueous acidic solution and their controlled releasing behavior with high biocompatibility are reported.

Experimental Part

Materials

The materials that were used in this work included chitosan (degree of deacetylation 85%, molecular weight = 190 kDa), lithium chloride (LiCl, 99%), pyridine (Py), dimethylformamide (DMF, 99%), 5-FU (99%) and IBU (99%), supplied by Sigma-Aldrich Chemical Co. Natural graphite flakes (325 mesh) were purchased from Alfa Aesar. All chemicals were used as received without further purification. FGOCs were synthesized in this work with reference to the literature.[16–21] First, GO was prepared using Hummer's method.[18] Then, the carboxylic acid groups of GO were converted into acyl chlorides (graphene-COCl) via standard chemistry, followed by a typical functionalization process for graphene with chitosan. More details on the synthesis are described in the Supporting Information.

Characterization

FT-IR spectra were recorded using a Spectrum GX. The scan wavenumber was in the range 600–4 000 cm^{-1} with a resolution of 1 cm^{-1}, and sixteen signals were averaged. Thermogravimetric analysis (TGA) was conducted under nitrogen on a TA instruments Q50 at a heating rate of 10 °C · min^{-1}. The WAXD measurements were performed using a conventional X-ray diffractometer [Rigaku Miniflex, Cu K_α, $\lambda = 1.5418$ Å]. The Raman spectra were recorded from 1 000 to 2 000 cm^{-1} using a FT Raman spectrometer (FRS-100S, Bruker) with an argon ion laser excitation of 514.5 nm. The XPS spectra were recorded using a VG-Scientific ESCALAB 250 spectrometer (UK) with a monochromatized Al K_α X-ray source. During the measurements, the base pressure was 1.33×10^{-7}–1.33×10^{-8} Pa. The binding energies were referenced to the C1s line at 284.6 eV from adventitious carbon. The survey spectra were obtained at a resolution of 1 eV from three scans. The atomic force microscopy (AFM) images of graphene were acquired in the tapping mode using a Multimode Nanoscope TM SPM, Digital Instruments (USA). The exfoliated surface morphology of the functionalized graphene (FGOCs) was measured using field emission scanning electron microscopy (FE-SEM, JSM-6700F, Korea Basic Science Institute) at an acceleration voltage of 20 kV with a Model 952888(8) microscope from Hitachi Ltd. UV absorption spectra were obtained using a UV-visible spectrophotometer (U-2010, HITACHI Co.). The fluorescence emission spectra were measured using a Hitachi F-4500 spectrometer at 25 °C. The excitation slit size was 10.0 nm and the emission slit size was also 10.0 nm. The scan speed was set at 240 nm · min^{-1}.

Drug Loading and Release

100 mg of FGOCs graphene sheets were dispersed in 25 mL/60 mg hexane/IBU or water/5-FU solutions. The mixtures were incubated for 48 h to fabricate drug loaded FGOCs sheets. Solutions were covered with a polyethylene (PE) film to prevent the evaporation of solvent. The drug loaded sample was separated from the solution by vacuum filtration, washed with solvent until complete removal of drugs was achieved and dried at room temperature. To check the removal of drugs from the FGOCs sheets, drug loaded FGOCs sheets were again washed with an appropriate solvent (hexane for IBU and water for 5-FU, respectively) and the filtrate was further measured using UV-vis spectrophotometry. The remaining drug loading amount was then also measured using UV-vis spectrophotometry. Then, 40 mg of drug loaded sample were dispersed in 5 mL of phosphate-buffered saline (PBS, pH = 7.4) and simulated stomach fluid (SSF, pH = 1.4), placed into a dialysis membrane bag (molecular-weight cutoff 5 000 kDa), and then immersed into 25 mL PBS and SSF, respectively, at 37 °C for 3 d.

At periodic intervals, the release media was withdrawn and another 1 mL of fresh buffer solution was added. The amounts of IBU and 5-FU were determined by means of measuring the UV-vis spectrum at 224 and 265 nm, respectively. The reason behind the use of the two kinds of release media (PBS and SSF) is the different nature of the drug molecules at different pHs, i.e., IBU has a pK_a of 4.43 and 5-FU has a pK_a of 8.2. Moreover, the pH-dependent drug release from FGOCs nanosheets is important in the clinical setting, since the microenvironment in the extracellular tissues of tumors and intracellular lysosomes and endosomes are acidic.[10]

Cell Proliferation Assays

The 3-(4,5-dimethylthiazol-2-yl)-2,5-diphenyltetrazolium bromide (MTT) assay was used to determine the cytotoxicity of neat GO, FGOCs and drug loaded FGOCs graphene sheets. Herein, we have tried two types of in vitro cancer cell line viability, namely CEM human lymphoblastic leukemia and MCF7-human breast cancer for targeting the potent cancer cell killing effect with different concentrations of each sample. Cell proliferation was measured using the MTT (Sigma-Aldrich Co., St. Louis, MO) colorimetric dye reduction method. The cells were seeded in tissue culture flasks (5×10^3 cells) and incubated in a fully humidified atmosphere containing 5% CO_2 at 37 °C. For MTT assays, the cells were seeded in

96 well plates at a density of 5×10^3 cells per well in 1 mL of culture medium, and then the cells were incubated with GO, FGOCs and drug loaded FGOCs sheets. It is pointed out here that we present the cell line viability of all samples for 5 d for both cell lines. This is because, for CEM human lymphoblastic leukemia, it was hard to know the toxic effect of FGOCs and drug loaded FGOCs sheets up to 3 d. In order to know the complete effect of the respective samples on both cell lines, therefore, we extended the cell proliferation assays to 5 d. The same trend was followed in the case of MCF-7 cell lines for reliable assessment.

After 5 d, the medium was aspirated after centrifugation and MTT-formazan crystals were solubilized in 100 μL dimethyl sulfoxide (DMSO). The optical density of each sample was measured at 570 nm using an ELISA reader (Bio-Tec Instruments, VT, USA). The optical density of the media was proportional to the number of viable cells. Inhibition of proliferation was evaluated as a percentage of control growth (no drug in the sample). All experiments were repeated at least twice.

Results and Discussion

Chitosan-Functionalized Graphene

Graphene oxide was prepared by oxidizing graphite via a modified Hummer's method.[18] The resulting GO (single layered and few-layered) was dispersible in water but aggregated in solution. The FGOCs were obtained from the chitosan and graphene oxide molecules, which were covalently bonded together via an amide bond (Scheme 1) in DMF in the presence of pyridine, following standard chemistry. The covalent attachment of chitosan onto GO via the amide linkage was confirmed using IR spectroscopy, TGA and XPS. In Figure 1(a), the peaks at 1 726 and 1 223 cm^{-1} in the FT-IR spectra were characteristic of the C=O and C−O stretches of the carboxylic and epoxy groups, respectively, on graphene oxide. In the FGOCs spectrum, the peak at 1 726 cm^{-1} almost disappeared, and a new broad band emerged at 1 653 cm^{-1}, corresponding to the C=O characteristic stretching band of the amide groups, which were further overlapped with C=O in the ester groups.[19,20] Moreover, a broad peak at 1 554 cm^{-1}, as well as two weak peaks at 1 167 and 806 cm^{-1}, presumably confirmed the N–H bending and C–N stretching bonds of the amide group. Additionally, the two characteristic bands of the glucopyranose rings of the FGOCs appeared at 897 and 1 115 cm^{-1}, respectively, implying that chitosan was attached.[21] The results from TGA in Figure 1(b) showed that three significant weight loss events were observed for GO powders, corresponding to the evaporation of water (below 100 °C) and the loss of what is likely to be carbon dioxide gas species (120–150 and 200–260 °C) from the decomposition of labile oxygen functional groups.[10] In contrast, the FGOCs have less than 2% weight loss below 100 °C. The gradual weight loss about 15% below 350 °C is likely to be due to the loss of the glucopyranose ring of

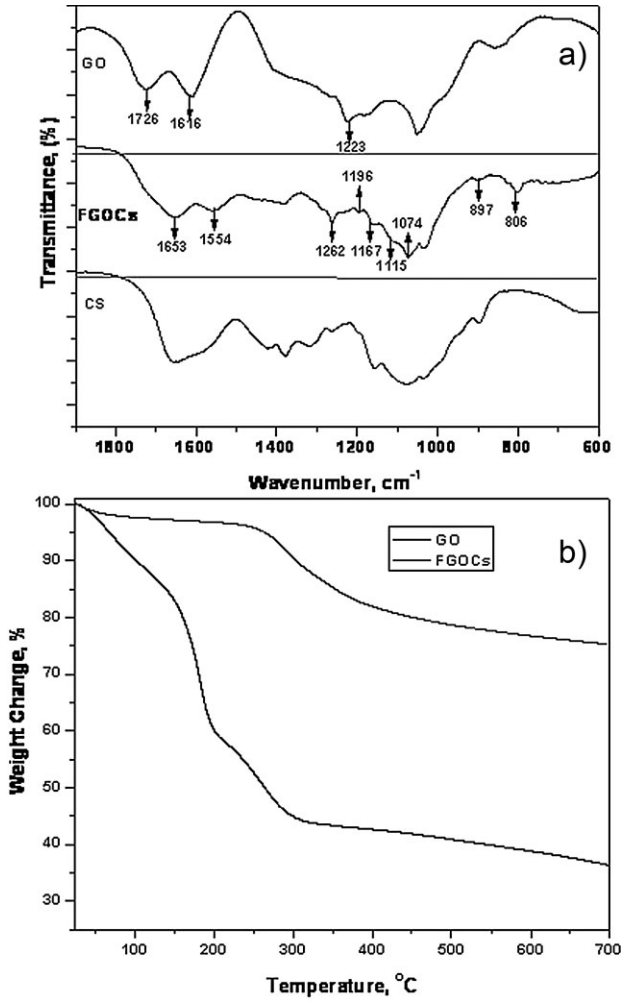

Figure 1. a) FT-IR spectra of GO, FGOCs, and CS and b) TGA curve of GO and FGOCs at a heating rate of 10 °C · min^{-1}.

chitosan and residual functional groups on the FGOCs sheets. These results are easy to understand: the oxidation product of GO has a layered morphology with oxygen-containing functionality, thereby weakening the van der Waals forces between layers. This will disrupt the hexagonal carbon basal planes on the interior of multi-layered stacks of GO, thus accelerating the process of weight loss, yielding CO, CO_2 and steam.[22] Remarkably, after functionalization of chitosan onto GO sheets, the total weight losses decreased to 42%, revealing that most of the epoxide and hydroxyl groups were successfully removed.

Figure 2 shows the C1s XPS spectra of GO and the FGOCs (for the XPS survey spectra of GO and functionalized graphene hybrid sheets, i.e., FGOCs, see Figure S1, Supporting Information). In the C 1s XPS spectrum of GO in Figure 2(a), four types of carbon were clearly present with different chemical valences. The C 1s peaks of the graphite's C−O, C=O and O−C=O were observed at 284.6, 286.7, 288.1

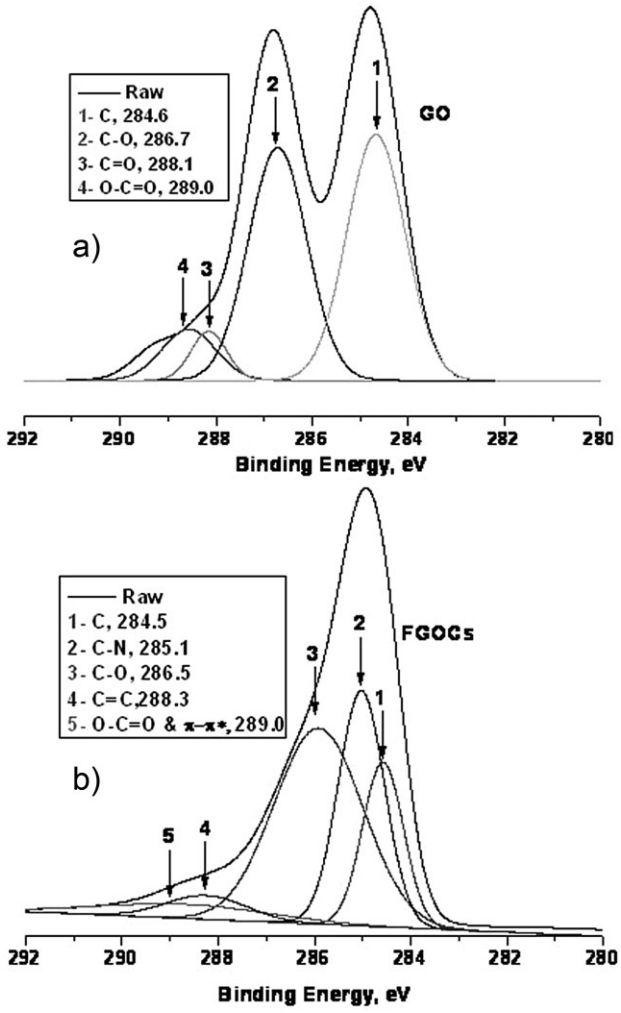

Figure 2. a) C 1S XPS spectra of GO and b) of FGOCs. The C 1s XPS spectra of GO and the FGOCs showed that four types of carbon were clearly present with different chemical valences.

and 289.0 eV. Although these four types of carbon were also present in the functionalized graphene, the C1s XPS spectrum of the FGOCs in Figure 2(b) clearly exhibited different intensity ratios. In contrast to the polymer reference (chitosan), an additional component at 285.1 eV, corresponding to the carbonyl (C—N) bond was observed in the C1s XPS spectrum of the FGOCs. Notably, the peak intensities of the oxidized carbon in the FGOCs were much lower than GO, and the C/O atomic ratio remarkably increased (from 1.72 to 4.6), indicating that most of the epoxide and hydroxyl groups disappeared after chemical modification by chitosan, suggesting that the GO was successfully modified.[23] Remarkably, a π-π^* transition took place in the basal plane after the reduction of the C1s peaks of O—C=O at 289.0 eV for the FGOCs. From these intensities, we can calculate the atomic percentages of the elements present after the functionalization procedure. This quantitative analysis is reported in Table S1 (Supporting Information) and shows a decrease of the oxygen levels and increase of the nitrogen levels.

The chitosan functionalization of graphene facilitated its exfoliation in the aqueous acidic solution. Note that results were given here only for aqueous acetic acid solution, but it is also possible to disperse FGOCs graphene sheets in other organic or inorganic aqueous acidic solutions. The GO dispersion with aqueous acetic acid was light brown, as shown in Scheme 1. However, a black graphene dispersion (0.1 mg/1 mL) was observed for the FGOCs. This clear color change of the dispersion before and after the chemical modification was apparent evidence that GO was indeed reduced after the covalent functionalization with chitosan. Additionally, the resulting graphene dispersion was stable for several days to a few months. The negative charges of the terminal carboxylic acid and protonated amine groups of chitosan were believed to supply an electrostatic repulsion, which provided stability for the graphene dispersions. Notably, after the addition of DMF into the solution (Figure S2, Supporting Information), the electrostatic repulsion was reduced, and graphene was recovered from the aqueous acetic solution.

Significant structural changes occurred during the chemical processing from the pristine graphite (Gy) to GO and finally to the FGOCs. In the Raman spectrum of the Gy, the peak at 1 580 cm^{-1} (G band) corresponded to the first order scattering of the E2g mode of the Gy in Figure 3(a) and was related to the vibration of the sp^2-bonded carbon atoms in a 2D hexagonal lattice. The (weak) disorder band that was caused by the Gy edges (D band) was observed at approximately 1 351 cm^{-1}. Comparing to the raw graphite, both the G and the D bands underwent significant changes to values of 1 601 and 1 354 cm^{-1} respectively, upon the amorphization of graphite. The GO peaks for amorphous carbon containing a certain fraction of sp^3 carbons became weaker and broader, suggesting a higher level of disorder in the graphene layers. The Raman spectrum of the FGOCs also contained G and D bands at 1 584 and 1 351 cm^{-1}, respectively. Along the Gy-GO-FGOCs path, although the G band peak was located at a higher frequency in GO than in graphite (1 601 vs. 1 580 cm^{-1}), the G band peaks were located at almost the same frequency in the FGOC and Gy. The blue shift, shifted to a higher frequency after the amorphization of graphite, can be explained by the transition from the graphite crystal to the single GO sheet.[24] In the FGOCs, the G band shifted back to the position of the G band in graphite, which was attributed to a graphitic "self-healing" that was similar as the decrease in the intensity of the D peak in heat-treated graphite.[25,26] The shoulder peak appearing at around 1 601 cm^{-1} also indicates that the FGOCs were partially reduced and a significant area in the FGOCs remained as its oxide form after the functionalization with chitosan.[27,28] The D/G intensity ratio of the FGOCs (1.44) increased compared to

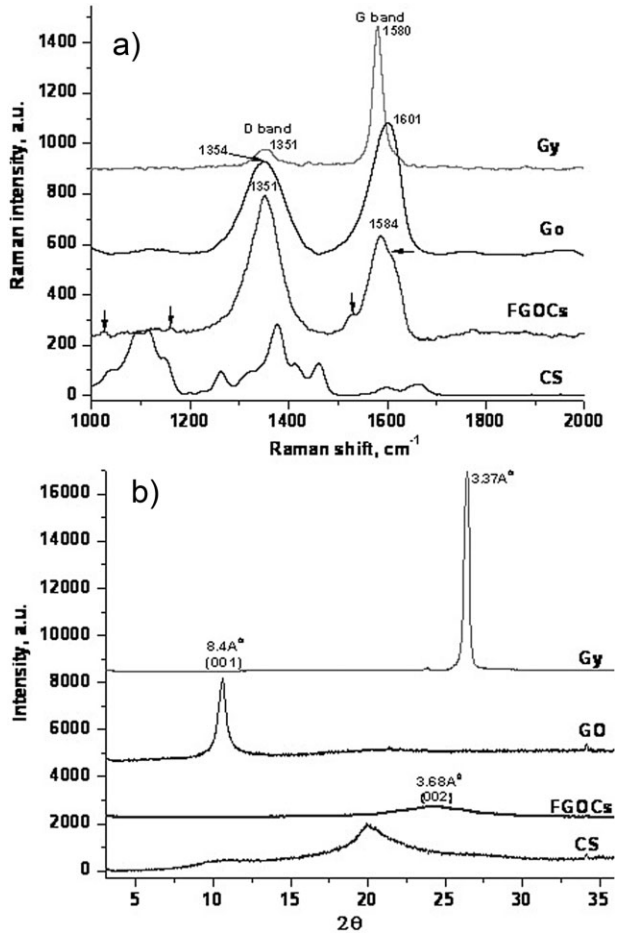

Figure 3. a) Raman spectra and b) X-ray diffraction patterns of pristine graphite (Gy), GO, FGOCs and CS.

that of GO (0.69), which means that the sp^3 carbon domain in the FGOCs increased with the functionalization of GO. Note that the covalent bonds between GO and chitosan might hinder the reduction of GO and the peak from chitosan chains can partially overlap with the D band of the FGOCs.[29] Furthermore, the arrow peaks that were presumably assigned to the Ag2 mode of chitosan were shifted by several wavenumbers compared to the pristine chitosan. This relative shift sufficiently suggested a strong interaction between chitosan and the graphene sheets.[22] The self-healing effect after the functionalization of GO with chitosan was further confirmed by wide angle X-ray diffraction [Figure 3(b)]. The pristine graphite nanosheet (Gy) exhibited a (002) diffraction peak at $2\theta = 26.45^\circ$, corresponding to a *d*-spacing of 3.37 Å in Figure 1(b), and the (001) peak of GO was located at $2\theta = 10.84^\circ$, corresponding to an interlayer distance of 8.4 Å. For the FGOCs, the highly broad diffraction peak [(002) plane], appearing at $2\theta = 24.16^\circ$, suggested that the interlayer distance of the FGOCs was slightly increased compared to that of pristine graphite and graphene layers of the FGOCs were partially exfoliated with a *d*-spacing of 3.68 Å. Additionally, the FGOCs exhibited an amorphous structure. The disruption in their structure and the significant reduction in the *d*-spacing suggested that attractive interactions existed between the layers, allowing this material to apply for drug carriers in addition to their excellent dispersibility in the solvents[30] (see Figure S2, Supporting Information).

Activation and functionalization of GO led to increases in optical absorption in the visible and near-infrared range. The optical absorption peak at 235 nm, originating from the π-plasmon of carbon,[31] remained essentially unchanged. The FGOCs showed much higher absorbance in the vis-NIR range than GO [Figure 4(a)]. The significant increase in absorbance led to a solution color change (darkening) that is visible to eye (Scheme 1, inset). Similar darkening was observed in the hydration reduction of GO, which is attributed to restoration of electronic conjugation within graphene sheets.[32,33] According to the AFM image in Figure 5, FGOCs contains monolayer graphene with a thickness of ≈1.85 nm and is greater than unmodified monolayers of GO, i.e., 1 nm. In the scanning electron microscopy (SEM) image (Figure S3, Supporting Information), the FGOCs possessed lateral dimensions ranging from several hundred nanometers to several micrometers and were arranged in an edge-to-edge configuration. Therefore, no significant folding or overlapping was observed.[10]

Restoration of electronic conjugation will reboot the aromatic basal planes on FGOCs and therefore is capable of absorbing aromatic compounds via inter/atomic interactions. This may be useful for drug carriers. Thus far, few reports have been published on the controlled loading and targeted delivery of two or more different drugs using graphene-based nanocarriers. Dai et al.[13] and Zhang et al.[34] have reported poly(ethylene oxide) (PEO) functionalized graphene for biological applications. However, both authors used doxorubicin, SN38 and CPT as model anticancer drugs, having a high density of π-electron clouds and more than two aromatic rings. These drugs are sometimes easy to attach onto the aromatic basal planes of functionalized GO on both sides by the hydrophobic and π-π stacking interaction. π-π interactions are caused by intermolecular overlap of p-orbitals in π-conjugated systems, so that they become stronger as the number of π-electrons increases. Other non/covalent interactions, including hydrogen bonds, van der Waals forces, charge/transfer interactions and dipole/dipole interactions, also attract organic moieties.

Drug Delivery

Until now, no reports have been published on drug molecules containing one aromatic moiety being loaded and their controlled release behavior through the graphene

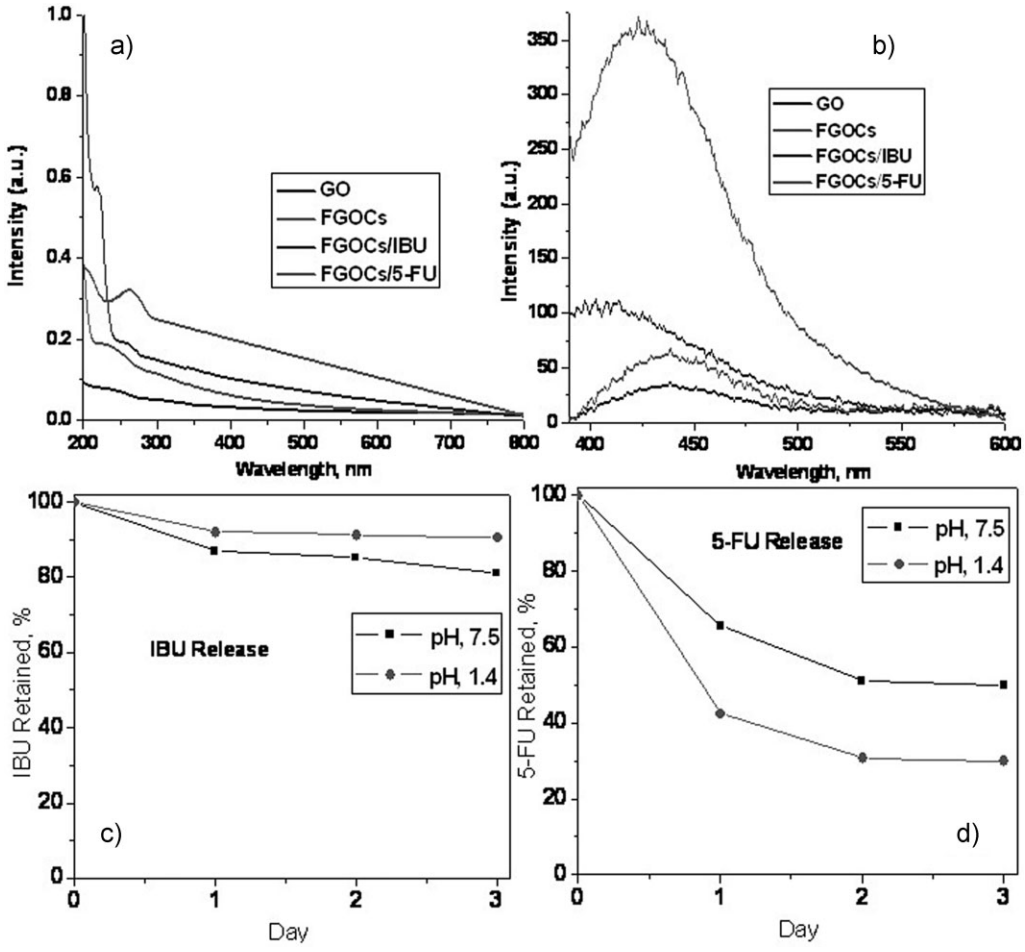

Figure 4. a) UV-vis absorbance spectra of GO, FGOCs and drug-loaded FGOCs. b) Fluorescence of GO and drug-loaded FGOCs in the visible range under excitation of 390 nm. c) IBU release and d) 5-FU release behavior of FGOCs/IBU and FGOCs/5-FU, respectively.

sheets. Herein, we have used an anti-inflammatory drug, ibuprofen ($pK_a = 4.43$) and an anti-cancer drug, 5-fluorouracil (5-FU, $pK_a = 8.2$) as model and widely useful drugs in biomedical applications.[35] IBU is an aromatic drug that will create hydrophobic and π-π interactions, whereas 5-fluorouracil, a "benzenoid" resonance contributor, is aromatic. It has a continuous loop of p orbitals (the two nitrogen are sp^2) and its "diamide" contributor obeys all preference rules. Thus, it is believed to be the best resonance contributor (see Figure S4, Supporting Information). In both cases, inter/atomic interactions will remain. An aromatic hydrophobic drug and hydrophilic drug were loaded onto the FGOCs via simple physisorption (Figure S5, Supporting Information). We found that an aromatic drug (IBU) and a hydrophilic drug (5-FU) were complexed with FGOCs via simple physisorption of IBU and 5-FU dissolved in hexane and water with FGOCs solution, respectively (Figure S5, Supporting Information). The excess and uncoupled drugs were removed by centrifugation. Repeated washing and filtration were used to remove residual free IBU and 5-FU through its respective solutions, i.e., hexane for IBU and water for 5-FU, respectively. We found that the FGOCs were highly stable in physiological solution including buffer (Figure S6, Supporting Information). We also investigated the cytotoxicity and completed cell viability tests of the FGOCs sheets. The excess and uncoupled drugs were removed by centrifugation. Repeated washing and filtration were used to remove residual free IBU and 5-FU. UV-vis spectra of the resulting solutions revealed IBU and 5-FU peaks superimposed with the absorption curve of FGOCs in Figure 4(a), suggesting loading of IBU and 5-FU onto FGOCs sheets. On the basis of the extinction coefficients, we estimated that the drug loading ratio of IBU on FGOCs sheets was $0.097\ mg \cdot mg^{-1}$ and higher than that of 5-FU ($0.053\ mg \cdot mg^{-1}$). The difference in the loading ability of the drugs is ascribed to the difference in their chemical structures and interactions with FGOCs. IBU is a kind of hydrophobic drug containing a complete aromatic ring and would create complete π-π interaction with aromatic basal planes of FGOCs. Furthermore, IBU can create hydrogen

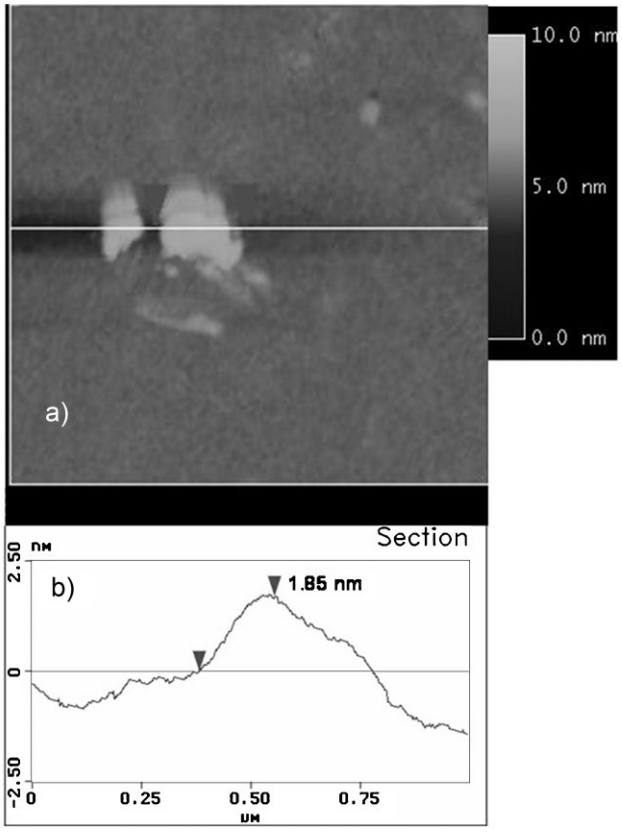

Figure 5. a) Tapping mode AFM image of functionalized graphene FGOCs, deposited on freshly cleaved mica substrate and b) cross-section analysis of FGOCs AFM image, i.e., (a).

bonding between the –COOH of IBU and the glucopyranose ring of chitosan. Meanwhile, 5-FU has a relatively hydrophilic character and its diamide group would contribute in the resonance of benzenoid and therefore the π-π interaction of 5-FU with FGOCs would be less, causing less loading of 5-FU on FGOCs sheets. From the fluorescence spectra of FGOCs/IBU, FGOCs/5-FU, FGOCs and GO at the same concentration ($0.1\,mg \cdot mL^{-1}$), a drastic increase of the fluorescence intensity was observed in FGOCs/IBU and FGOCs/5-FU compared to in GO and FGOCs, as shown in Figure 4(b). This result suggests the close proximity of the drug molecule with FGOCs through non-covalent bonding of drug on FGOCs sheets.[36] The release of drugs from FGOCs sheets was carried out in PBS (pH = 7.4) and SSF (pH = 1.4) at 37 °C.

We observed from Figure 4(c) that IBU was released only ≈10% in SSF from FGOCs nanosheets, whereas the release rate was increased up to 70% into the respective release medium for 5-FU in 3 d, as shown in Figure 4(d). The same trend was observed in the release rate of both drugs for the PBS releasing medium. Here, IBU was released up to ≈19% only but, unlike IBU, 5-FU was released up to 50%. The significantly different IBU release behavior from FGOCs graphene sheets under pH stimulation can be mainly attributed to the interaction of IBU with FGOCs and ionization of IBU at different pH values.

In both cases, the interaction of IBU with FGOCs would be same regardless of pH but at pH = 7.5 IBU would be ionized ($pK_a = 4.43$), causing a higher release than that at pH = 1.4, whereas at pH = 1.4 IBU would be deionized and exhibit less release. At pH = 7.5, the release rate of 5-FU becomes slower than that at pH = 1.4, because 5-FU would be protonated at pH = 1.4 (amine group) causing more easy release from FGOCs graphene sheets. Moreover, as mentioned above, IBU has a more hydrophobic and stronger π-π staking interaction with FGOCs than 5-FU and therefore IBU has more distinct controlled release behavior.

We found that FGOCs/5-FU sheets afforded highly potent cell viability from 93.4 to 30.1% at 10 to $400\,\mu g \cdot mL^{-1}$ concentration with the CEM cell line after being incubated for 5 d, as shown in Figure 6(a). Consistency of cell line viability was almost the same in FGOCs/IBU samples. Importantly, no serious toxicity of the CEM cell line was measured for various concentrations of FGOCs graphene sheets without drug loading, suggesting that FGOCs sheets had very good biocompatibility.

5-Fluorouracil is a widely used chemotherapy drug for targeting various cancers. 5-FU loaded graphene sheets (FGOCs/5-FU) again induced significant MCF-7 cancer cell

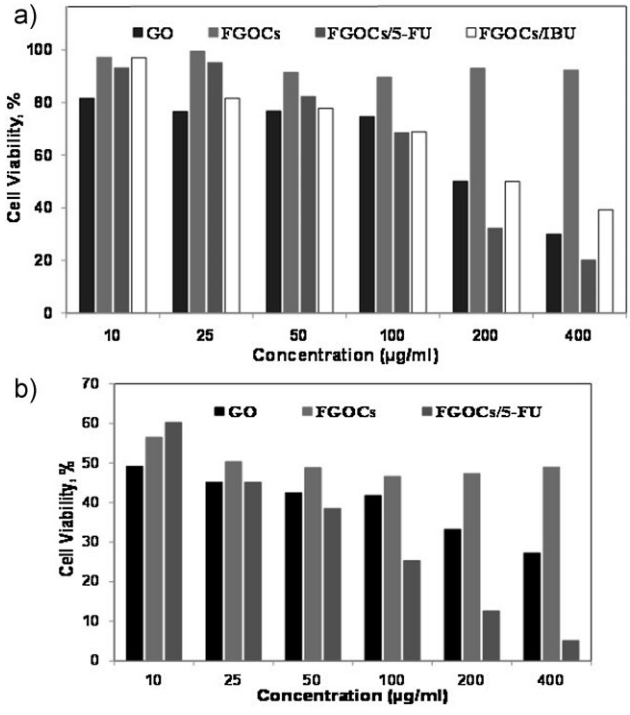

Figure 6. In vitro cell viability assay. a) Relative cell viability of CEM cancer cell line and b) MCF-7 cancer cell line incubated with GO, FGOCs, and drug loaded FGOCs graphene sheets at different concentrations for 5 d (SD ± 3%).

death, as shown in Figure 6(b). We suggest that 5-FU-loaded FGOCs sheets transported 5-FU inside the cells via endocytosis. One of the potential advantages of using FGOCs as a drug carrier compared to free drug is the ability to target delivery for selective destruction of certain types of cells, reducing the toxicity to non-targeted cells. It was found that 5-FU loaded FGOCs exhibited higher concentration-dependent toxicity (10 to 100 $\mu g \cdot mL^{-1}$) to MCF cells than FGOCs and GO sheets, suggesting that chitosan conjugation to graphene sheets afforded no enhancement in 5-FU delivery to MCF cells. These results suggest the potential for selectively enhancing the toxicity of drugs to certain types of cells by using FGOCs sheets with a targeting moiety as drug carriers. It is worth pointing out that we found targeting cell killing anti-cancer drug loaded graphene sheets having high and long term biocompatibility (5 d) with different kind of cancer cell lines (CEM & MCF-7). Moreover, FGOCs sheets exhibit higher (≈20%) biocompatibility than GO sheets for both cell lines.

A drug delivery system is generally designed to improve the pharmacological and therapeutic profile of a drug molecule. The ability of FGOCs to penetrate into the cells offers the potential to use FGOCs as vehicles for the delivery of drug molecules. Delivery systems should be able to carry one or more therapeutic agents with recognition capacity and optical signals for imaging and/or specific targeting that is of fundamental advantage, for example, in the treatment of cancer and different types of infectious diseases. For this purpose, we have developed a new strategy for the functionalization of GO with chitosan. For future applications of FGOCs, it may be useful for clinical applications to incorporate a fluorescent probe into the FGOCs for tracking the cellular uptake of the material and an antibiotic moiety as the active molecule which can covalently link to FGOCs.

It is well known that carbon nanotubes (CNT) can be imaginatively produced by rolling up a single layer of graphene sheet (single-walled CNT, SWCNT)[36,37] and by rolling up many layers to form concentric cylinders (multi-walled CNT, MWNT)[38] which show promise as materials for in vivo delivery and imaging applications.[39–43] Besides CNT having a specific emphasis in biological applications, graphene is currently an intensively investigated material for the same applications. In the present work, we have disclosed in vitro testing of both drug delivery and cell line studies of FGOCs. It may be useful as an in vivo administrated vehicle for drugs via intravenous therapy and oral administrations. Recently, Liu et al. have published a paper related to the in vivo behavior of nanographene sheets (NGS) with poly(ethylene glycol) (PEG) coating by a fluorescent labeling method using Cy7 dye for in vivo tumor uptake and efficient photothermal therapy.[44] They have mentioned that Cy7 dye was covalently conjugated to nanographene sheets via the formation of an amide bond instead of physical absorption by π-stacking. The same trend can be applied to our FGOCs as a future administrator. Moreover, using ^{64}Cu and ^{60}Co labeling, FGOCs may be useful as in vivo administrated vehicles for drugs via intravenous therapy, since chitosan is a well known biopolymer for in vivo treatment.[45–47]

Conclusion

In summary, GO was successfully functionalized with chitosan. The excellent exfoliation and dispersion of the functionalized graphene sheets in the aqueous acetic acid solution presented here suggests that this method could be used to produce exfoliated, reduced graphene sheets. Moreover, IBU and 5-FU were loaded successfully on FGOCs sheets, despite lower numbers of π electrons. Controlled release behavior and long term biocompatibility of FGOCs graphene sheets suggest that these graphene sheets are promising novel materials for biomedical applications. This facile and low cost process could improve the commercial applications of graphene materials.

Acknowledgements: This work was supported by the *National Research Foundation of Korea* (NRF) through the *Acceleration Research Program* (No. 20100000790), the *Pioneer Research Center Program* (2010-0019308/2010-0019482), the *WCU program*, and *Brain Korea 21 Project* funded by the *Ministry of Education, Science and Technology, Korea*.

Received: August 20, 2010; Revised: October 20, 2010; Published online: December 22, 2010; DOI: 10.1002/mame.201000307

Keywords: biocompatibility; chitosan; drug delivery systems; functionalization of polymers; solution properties

[1] A. K. Geim, K. S. Novoselov, *Nat. Mater.* **2007**, *6*, 183.
[2] X. L. Li, X. R. Wang, L. Zhang, S. W. Lee, H. J. Dai, *Science* **2008**, *319*, 1229.
[3] K. S. Novoselov, A. K. Geim, S. V. Morozov, D. Jiang, M. I. Katsnelson, I. V. Grigorieva, S. V. Dubonos, A. A. Firsov, *Nature* **2005**, *438*, 197.
[4] Y. Zhang, J. W. Tan, H. Stormer, L. P. Kim, *Nature* **2005**, *438*, 201.
[5] N. Tombros, C. Jozsa, M. Popinciuc, H. T. Jonkman, B. J. van Wees, *Nature* **2007**, *448*, 571.
[6] K. S. Kim, Y. Zhao, H. Jang, S. Y. Lee, J. M. Kim, K. S. Kim, J.-H. Ahn, P. Kim, J. Choi, B. H. Hong, *Nature* **2009**, *457*, 706.
[7] Y. Wang, Y. Huang, Y. Song, X. Y. Zhang, Y. F. Ma, J. J. Liang, Y. S. Chen, *Nano Lett.* **2009**, *9*, 220.
[8] D. C. Elias, R. R. Nair, T. M. G. Mohiuddin, S. Morozov, V. P. Blake, M. P. Halsall, A. C. Ferrari, D. W. Boukvalov, M. I. Katsnelson, A. K. Geim, K. S. Novoselov, *Science* **2009**, *323*, 610.

[9] M. F. Yu, O. Lourie, K. Moloni, T. F. Kelly, R. S. Ruoff, *Science* **2000**, *287*, 637.
[10] Y. Zhu, M. D. Stoller, W. Cai, A. Velamakanni, R. D. Piner, D. Chen, R. S. Ruoff, *ACS Nano* **2010**, *4*, 1227.
[11] S. H. Lee, D. R. Dreyer, J. An, A. Velamakanni, R. D. Piner, S. Park, Y. Zhu, S. O. Kim, C. W. Bielawski, R. S. Ruoff, *Macromol. Rapid Commun.* **2010**, *31*, 281.
[12] A. Chunder, J. Liu, L. Zhai, *Macromol. Rapid Commun.* **2010**, *31*, 380.
[13] X. Sun, Z. Liu, K. Welsher, J. T. Robinson, A. Goodwin, S. Zaric, H. Dai, *Nano Res.* **2008**, *1*, 203.
[14] Z. Liu, J. T. Robinson, X. Sun, H. Dai, *J. Am. Chem. Soc.* **2008**, *130*, 10876.
[15] M. N. V. Ravi Kumar, R. A. A. Muzzarelli, C. Muzzarelli, H. Sashiwa, A. J. Domb, *Chem. Rev.* **2004**, *104*, 6017.
[16] X. Yang, Y. Tu, L. Li, S. Shang, X.-M. Tao, *ACS Appl. Mater. Int.* **2010**, *2*, 1707.
[17] D. Han, L. Yan, W. Chen, W. Li, *Carbohydrate Polym.* **2011**, *83*, 653.
[18] S. Hummers, R. E. Offeman, *J. Am. Chem. Soc.* **1958**, *80*, 1339.
[19] S. Niyogi, E. Bekyarova, M. E. Itkis, J. L. McWilliams, M. A. Hamon, R. C. Haddon, *J. Am. Chem. Soc.* **2006**, *128*, 7720.
[20] X. Zhang, Y. Huang, Y. Wang, Y. Ma, Z. Liu, Y. Chen, *Carbon* **2008**, *47*, 313.
[21] G. Ke, W. Guan, C. Tang, W. Guan, D. Zeng, F. Deng, *Biomacromolecules* **2007**, *8*, 322.
[22] J. Shen, Y. Hu, M. Shi, N. Li, H. Ma, Ye. Mingxin, *J. Phys. Chem. C* **2010**, *114*, 1498.
[23] X. Fan, W. Peng, Y. Li, S. Wang, G. Zhang, F. Zhang, *Adv. Mater.* **2008**, *20*, 4490.
[24] R. Tuinstra, J. L. Koenig, *J. Chem. Phys.* **1970**, *53*, 1126.
[25] C. C. Han, J. T. Lee, H. Chang, *Chem. Mater.* **2001**, *13*, 4180.
[26] K. Sato, R. Saito, Y. Oyama, J. Jiang, L. G. Cancado, M. A. Pimenta, A. Jorio, G. G. Samsonidze, G. Dresselhaus, M. S. Dresselhaus, *Chem. Phys. Lett.* **2006**, *427*, 117.
[27] A. C. Ferrari, J. Robertson, *Phys. Rev. B* **2000**, *61*, 14095.
[28] D. Graf, F. Molitor, K. Ensslin, C. Stampfer, A. Jungen, C. Hierold, L. Wirtz, *Nano Lett.* **2007**, *7*, 238.
[29] K. N. Kudin, B. Ozbas, H. C. Schniepp, R. K. Prud'homme, I. A. Aksay, R. Car, *Nano Lett.* **2008**, *8*, 36.
[30] M. J. McAllister, J. L. Li, D. H. Adamson, H. C. Schniepp, A. A. Abdala, J. L. Xo, M. Herrera-Alonso, D. L. Milius, R. Car, R. K. Prud'homme, I. A. Aksay, *Chem. Mater.* **2007**, *19*, 4396.
[31] S. Attal, R. Thiruvengadathan, O. Regev, *Anal. Chem.* **2006**, *78*, 8098.
[32] S. Stankovich, D. A. Dikin, G. H. B. Dommett, K. M. Kohlhaas, E. J. Zimney, E. A. Stach, R. D. Piner, S. T. Nguyen, R. S. Ruoff, *Nature* **2006**, *442*, 282.
[33] I. Jung, D. A. Dikin, R. D. Piner, R. S. Ruoff, *Nano Lett.* **2008**, *8*, 4283.
[34] L. Zhang, J. Xia, Q. Zhao, L. Liu, Z. Zhang, *Small* **2010**, *6*, 537.
[35] S. J. Son, X. Bai, S. B. Lee, *Drug Discovery Today* **2007**, *12*, 650.
[36] Z. Liu, X. Sun, N. Nakayama, H. Dai, *ACS Nano* **2007**, *1*, 50.
[37] S. Iijima, T. Ichihashi, *Nature* **1993**, *363*, 603.
[38] D. S. Bethune, C. H. Klang, M. S. de Vries, G. Gorman, R. Savoy, J. Vazquez, R. Beyers, *Nature* **1993**, *363*, 605.
[39] V. L. Colvin, *Nat. Biotechnol.* **2003**, *21*, 1166.
[40] Z. Li, T. Hulderman, R. Salmen, R. Chapman, S. S. Leonard, S. H. Young, A. Shvedova, M. I. Luster, P. P. Simeonova, *Health Perspect.* **2007**, *115*, 377.
[41] A. Bianco, K. Kostarelos, M. Prato, *Curr. Opin. Chem. Biol.* **2005**, *9*, 674.
[42] L. Ma Hock, S. Treumann, V. Strauss, S. Brill, F. Luizi, M. Mertler, K. Wiench, A. O. Gamer, B. van Ravenzwaay, R. Landsiedel, *Toxicol. Sci.* **2009**, *112*, 468.
[43] Y. Sakamoto, D. Nakae, N. Fukumori, K. Tayama, A. Maekawa, K. Imai, A. Hirose, T. Nishimura, N. Ohashi, A. Ogata, *J. Toxicol. Sci.* **2009**, *34*, 65.
[44] K. Yang, S. Zhang, G. Zhang, X. Sun, S.-T. Lee, Z. Liu, *Nano Lett.* **2010**, *10*, 3318.
[45] Y. Bai, Y. Zhang, J. Zhang, Q. Mu, W. Zhang, E. R. Butch, S. E. Snyder, B. Yan, *Nature Nanotechnol.* **2010**, *5*, 683.
[46] G. Levitskaia, J. A. Creim, T. L. Curry, T. Luders, J. E. Morris, S. I. Sinkov, A. D. Woodstock, K. D. Thrall, *Health Phys.* **2009**, *2*, 115.
[47] X. L. Zhao, K. X. Li, X. F. Zhao, D. H. Pang, D. W. Chen, *Chem. Pharm. Bull. (Tokyo)* **2008**, *7*, 963.